Flow, Turbulence and Combustion (2023) 111:201–209
https://doi.org/10.1007/s10494-023-00410-9

BRIEF REPORT

Model assessment of synthetic jets for turbulent combustion experiments

Nicholas E. Thornburg[1] · Xuhui Feng[1] · Bradley T. Zigler[1] · Marc S. Day[2] · Shashank Yellapantula[2] · Sreekant Narumanchi[1]

Received: 31 August 2022 / Accepted: 16 March 2023 / Published online: 28 March 2023

Abstract

Understanding turbulent premixed flames is essential to predict and optimize advanced combustion strategies, but critical capability gaps exist for collecting and validating measurements such as turbulent flame speed. Here, we evaluate synthetic jets as a new, promising turbulence generation device for constant-volume combustion chambers, quantitatively assessing turbulence intensity and spatial uniformity in a hypothetical 4,189-cm^3 vessel for various premixture conditions.

Graphic Abstract

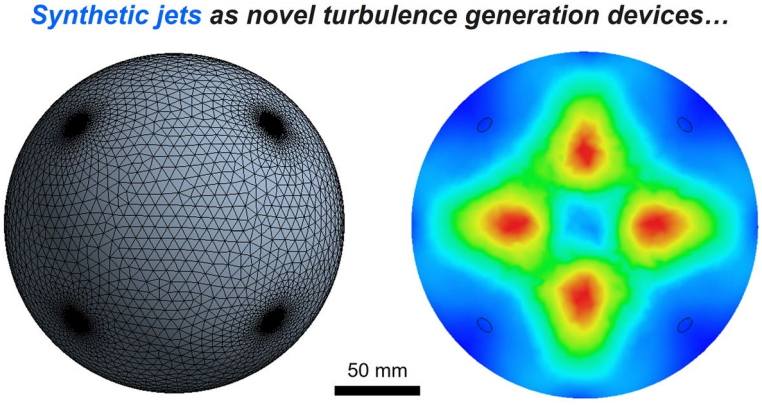

Keywords Flame speed · Synthetic jet · Turbulence · Combustion · Computational fluid dynamics

Nicholas E. Thornburg and Xuhui Feng have contributed equally to this work.

✉ Nicholas E. Thornburg
Nicholas.Thornburg@nrel.gov

Extended author information available on the last page of the article

1 Introduction

Laminar flame speed, also known as unstrained burning velocity, is an important fundamental property of flames, key to understanding fuel utilization and optimizing combustion efficiency. In the presence of turbulence, flame surfaces can be distorted, resulting in increased volumetric flame surface density as well as modifications to the local combustion chemistry. As a result, turbulent flame speed can be dramatically different than its laminar counterpart and hence serves a separate and distinct role in combustors. For internal combustion engines and turbines, high laminar flame speeds enable strong flame kernel development that is resistant to localized extinction, while high turbulent flame speeds allow the fuel to be consumed before end-gas conditions reach autoignition (i.e., knock). However, a significant capability gap exists for collecting and interpreting turbulent flame speed measurements. Such data are scant in the literature (Bradley et al. 2013; Bagdanavicius et al. 2015; Marshall et al. 2017; Turner et al. 2019) and lack sufficient generality to inform and validate predictive models (Farrell et al. 2004; Daniele et al. 2011) of turbulent flame phenomena across a broad range of device configurations.

Experimentally, turbulent flame speeds are typically measured using up to four canonical configurations: Bunsen flames, rod-stabilized flames, counterflow (stagnation) flames and spherically expanding flames (Law 2006). The first three of these feature stationary flames, while the final one requires dedicated devices capable of generating turbulence inside a spherical constant-volume combustion chamber (CVCC). CVCC facility surveys have been summarized elsewhere (Ravi et al. 2012). Generally, most turbulent CVCCs employ impellers (Ravi et al. 2012; Bradley et al. 2019; Mannaa et al. 2019; Morones et al. 2019) for relatively uniform turbulence generation, although recent reports suggest that traditional jets (i.e., nozzles) may also be used to create highly uniform turbulence (Davani and Ronney 2017; Davani et al. 2019). However, each experimental agitation method has unique limitations, such as vortical biases induced by impellers (Bonhomme et al. 2014; Bradley et al. 2019; Mannaa et al. 2019) or the pumping challenges (i.e., high pressure drop) required by the small openings of jet nozzles. Likewise, significant safety hazards are introduced by improper sealing and wear of high-rpm impeller parts, or, in the case of traditional jets, by the practical challenge of needing to premix the fuel and oxidizer in the absence of incidental ignition sources prior to entering the CVCC.

In this article, we explore the possibility of synthetic jets as an alternative and potentially advantaged turbulence generation device for turbulent combustion experiments. Unlike traditional jets, synthetic jets move fluid via periodically oscillating diaphragms that are contained within a wall-recessed cavity and eject fluid through a narrowed opening into the chamber (Smith and Swift 2003). Thus, synthetic jets result in high fluid ejection velocities with net-zero mass flux, driven by a significant momentum flux—attractive features for several applications encompassing power electronics cooling (Mahalingam and Glezer 2004; Arik et al. 2012; He et al. 2015), aerodynamics (Hassan and JanakiRam 1998; McCormick 2000), microfluidic devices (Mautner 2004) and granular flows (Han et al. 2020), among others. Turbulent premixing for combustion is one possible extension of synthetic jets, and we assess their technical viability as turbulence generation devices in a hypothetical 4,189-cm^3 CVCC using computational fluid dynamics (CFD) modeling. This model framework serves as an early basis for synthetic jet design and engineering for next-generation flame speed measurement apparatuses.

Table 1 Baseline system parameters and conditions for synthetic jet models (parenthetical values denote the additional conditions evaluated in this study)

Parameter	Assigned value
Temperature, T	300 (600) K
Pressure, P	1.0 (30) atm
Equivalence ratio, φ	1.0 (0.25, 1.25)
Mass fraction of methane, x_{CH4}	0.055
Mass fraction of oxygen, x_{O2}	0.220
Mass fraction of nitrogen, x_{N2}	0.725
Average fluid density[a], ρ	1.24 kg·m^{-3}
Chamber diameter, d_{ch}	200 (400, 800) mm
Slit diameter, d_{sl}	10 (5, 20) mm
Number of synthetic jets, N	8 (4, 20)
Velocity constant, v_0	10 (1, 20) m·s^{-1}
Oscillation frequency, f	500 (50, 100, 250, 1,250, 2,500) Hz
Mesh element length	0.0050 m for chamber domain, 0.0010 m for jet inlet region

[a]Ideal gas law assumed as the equation of state to calculate fluid mixture density

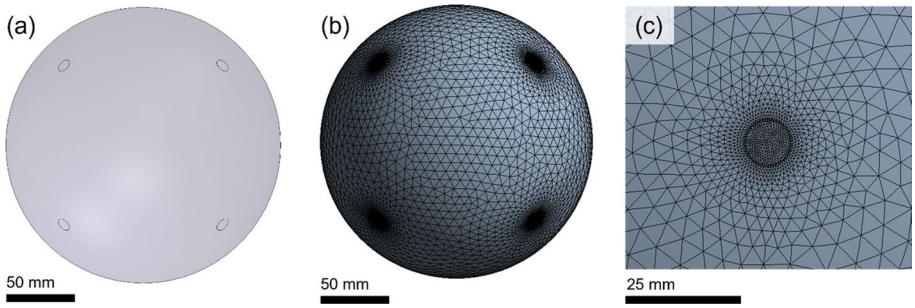

Fig. 1 **a** Illustration of three-dimensional spherical model control volume. Small circles at the surface represent 10-mm synthetic jet openings; four additional jets are symmetrically and oppositely located on the backside of the sphere (not shown). **b** Meshing of control volume, with refined finite volume sizing at and near jet openings. **c** Magnified illustration showing finer meshing at a jet opening

2 Results and Discussion

To assess the agitation behavior of a premixed fuel in air, we first define the appropriate system size, geometry and conditions to establish a synthetic jet modeling framework (Table 1). A stoichiometric ($\varphi = 1.0$) mixture of methane (CH_4) and air is assumed as a base-case fluid initially dispersed within a 200-mm-diameter spherical chamber (4,189-cm^3 volume). The eight synthetic jets are placed at the corners of a cube inscribed inside of the chamber (Fig. 1), a basis of configuration selected from prior studies on synthetic (Hwang and Eaton 2004) and traditional (Davani and Ronney 2017) jets. Further, the 10-mm-wide synthetic jets are "cavityless" (Fig. 1a), such that the fluid in the chamber is subjected to a periodic velocity boundary condition at the jet opening (Eq. 1), accomplishing net-zero mass flux without needing to define an explicit cavity geometry (Kral et al. 1997; Matiz-Chicacausa and Lopez Mejia 2020). (Notably, cavity shape, depth and internal volume are expected to significantly

influence the behavior of a real experimental device (Kotapati et al. 2007; Chaudhari et al. 2008, 2009; Jain et al. 2011; Capuano et al. 2019), but these considerations are beyond the scope of this study.)

Transient, finite-volume simulations are performed in ANSYS Fluent 2021 R2 to spatially discretize and solve the governing Reynolds-Averaged Navier–Stokes (RANS) equations using a shear stress transport (SST) k-omega (k–ω) turbulence model. We employ pressure–velocity coupling to compute the conservation equations via a segregated, guess-and-correct method and enable data sampling for time-based turbulence statistics (see Eqs. S1–S3 and discussion below). Full details of model development, sampling and sensitivity are included in the Supplementary Information (SI). To begin characterizing synthetic jet behavior predicted by this model framework, the root mean square (RMS) jet velocity v_{RMS} is calculated from Eq. (1) to describe a nominal average of synthetic jet velocities v from periodic fluid pulses of frequency f and amplitude v_0; this metric enables comparison to traditional jet behavior (Davani and Ronney 2017).

$$v = v_0 \sin(2\pi f t) \tag{1}$$

First, a 2D circular cut plane with four symmetrically opposed synthetic jets is employed as a simplified, reduced-order test case for the eight-jet 3D spherical volume to verify reasonable velocity profiles and an appropriate turbulence model (i.e., SST k–ω). Briefly, the CFD model conditions and parameters shown in Table 1 yield physically meaningful velocity profiles and turbulence intensities within expected orders of magnitude (Fig. S1), suggesting that the assumed physics models are valid for this system and may be readily extended to the 3D system (Fig. 1). Full details and discussion of assumptions and sensitivities (Roache 1994) are included in SI.

Turbulence magnitudes and uniformity metrics are derived from time-averaged sampling calculations of the mean velocity $\overline{u_{j,i}}$ (Eq. S1) and the RMS of fluctuating velocities $u'_{j,i}$, where j=x, y, z Cartesian coordinates at location i, allowing for calculation of time-averaged (Eq. S2) and volume-averaged (Eq. S3) turbulence intensities u'_i and $\overline{u'_V}$, respectively. Simulation times are sufficiently long to allow for at least 25 jet pulses. Following the volume-averaged quantitative analyses described by others (Davani and Ronney 2017), we similarly define the mean flow index (MFI), homogeneity index (HI) and isotropicity index (II) in Eqs. 2–4. Full definitions and discussion of index terminology are provided in SI.

$$MFI \equiv \frac{\sqrt{\frac{1}{V}\sum_{i=1}^{n}\left(\overline{u_i}\right)^2 v_i}}{\overline{u'_V}} \tag{2}$$

$$HI \equiv \frac{\sqrt{\frac{1}{3V}\sum_{i=1}^{n}\left[\left(u'_{x,i}-\overline{u'_V}\right)^2+\left(u'_{y,i}-\overline{u'_V}\right)^2+\left(u'_{z,i}-\overline{u'_V}\right)^2\right]v_i}}{\overline{u'_V}} \tag{3}$$

$$II \equiv \frac{\sqrt{\frac{1}{3V}\sum_{i=1}^{n}\left[\left(u'_{x,i}-u'_i\right)^2+\left(u'_{y,i}-u'_i\right)^2+\left(u'_{z,i}-u'_i\right)^2\right]v_i}}{\overline{u'_V}} \tag{4}$$

Briefly, MFI represents a volume-averaged RMS flow normalized by the volume-averaged turbulence intensity. HI represents the extent to which turbulence intensity remains constant within the entire control volume, whereas II represents the spatial uniformity of the local intensity values. All three turbulence metrics, along with $\overline{u_i}$ and $u_i^{'}$, are used here to characterize synthetic jet agitation effectiveness and uniformity for various test cases.

Figure 2 depicts the 3D model velocity fields resulting from simulation at conditions described by Table 1. These heat maps of velocity magnitude illustrate spatially symmetric fluid velocity profiles at the middle section plane within the chamber, suggesting that synthetic jets are capable of highly uniform agitation. Time-averaged turbulence statistics are reported in Table 2 for this base case (No. 2) and for variations of the velocity constant v_0 (Eq. 1), oscillation frequency f, methane/air equivalence ratio φ, synthetic jet slit size d_{sl}, and chamber diameter d_{ch}.

Overall, $\overline{u_i}$ and $u_i^{'}$ monotonically increase with increasing v_0, v_{RMS} and d_{sl} (Nos. 1–3, 11, 13), while f exhibits an inverse relationship with these two turbulence descriptors (Nos. 2, 4–8). When the total mass flowrate is kept constant with changing d_{sl} (Nos. 2, 12, 14), similar $\overline{u_i}$ and $u_i^{'}$ are calculated for the 5-, 10- and 25-mm openings, with some loss in turbulence intensity noted for the 25-mm case; relatedly, as d_{ch} is increased two-fold (No. 15) and four-fold (No. 16), time-averaged turbulence statistics precipitously decrease for a given fixed timescale. However, across all these cases, maximum local Reynolds numbers Re_{max} (Eq. S4) are identical within two significant figures for these three trials. Indeed, both d_{sl} and d_{ch} appear to be important yet flexible design parameters, potentially allowing for tunable flow profiles and extents of turbulence in a prospective real device. Finally, base-case RANS results (No. 2) are compared to predictions of a large eddy simulation (LES; No. 17), an alternate turbulence model which yields internally agreeable values for $\overline{u_i}$, $u_i^{'}$ and Re_{max}. Sensitivities of other model parameters are further assessed to verify the robustness of the 3D model relative to baseline model conditions and to a traditional jet analogue; full results are described in SI (Figs. S2–S4, Table S1).

Next, Fig. 3 illustrates calculated volume-averaged turbulence metrics as a function of dimensionless radial position r/R and oscillation frequency f for the base-case velocity constant v_0 of 10 m·s^{-1}. Above 50 Hz, turbulence indices MFI (Eq. 2, Fig. S5), HI (Eq. 3, Fig. 3a), II (Eq. 4, Fig. 3b) and time-averaged turbulence intensity $u_i^{'}$ (Eq. S2, Fig. S6) are

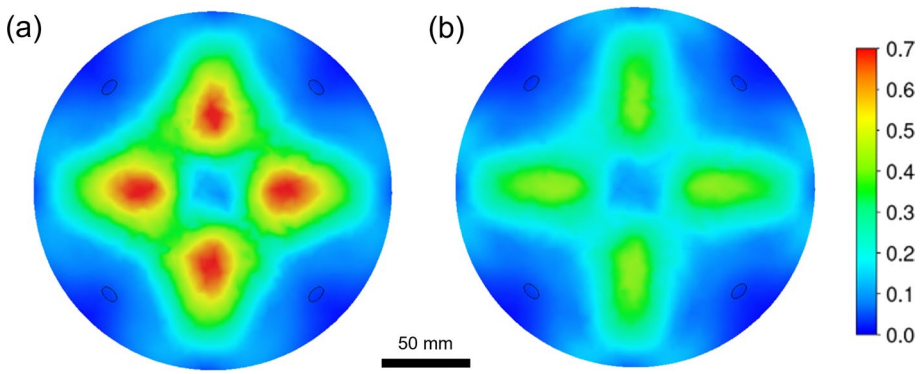

Fig. 2 Center-plane contours of 3D model results of **a** time-averaged mean velocity $\overline{u_i}$ (m·s^{-1}) and **b** time-averaged turbulence intensity $u_i^{'}$ (m·s.$^{-1}$). Color legend (right) illustrates magnitudes of each calculated velocity. See Table 1 for baseline conditions and Eqs. S1–S2 for definitions of $\overline{u_i}$ and $u_i^{'}$

Table 2 Summary of results of base case (No. 2, Table 1) and varied parameters

No	d_{sl} (mm)	d_{ch} (mm)	v_0 (m·s^{-1})	v_{RMS} (m·s^{-1})	φ	f (Hz)	$\overline{u}$(m·s^{-1})	u'(m·s^{-1})	Re_{max}
1	10	200	1	0.7	1.0	500	0.003	0.004	650
2	10	200	10	7.1	1.0	500	0.22	0.11	6,400
3	10	200	20	14	1.0	500	0.56	0.33	13,000
4	10	200	10	7.1	1.0	50	0.36	0.19	6,400
5	10	200	10	7.1	1.0	100	0.32	0.18	6,400
6	10	200	10	7.1	1.0	250	0.24	0.14	6,400
7	10	200	10	7.1	1.0	1,250	0.19	0.11	6,400
8	10	200	10	7.1	1.0	2,500	0.21	0.11	6,400
9	10	200	10	7.1	0.25	500	0.21	0.10	6,400
10	10	200	10	7.1	1.25	500	0.22	0.10	6,400
11	5	200	10	7.1	1.0	500	0.071	0.043	3,200
12	5*	200	20	14	1.0	500	0.23	0.12	6,400
13	25	200	10	7.1	1.0	500	0.36	0.28	16,000
14	25*	200	4	2.8	1.0	500	0.11	0.07	6,400
15	10	400	10	7.1	1.0	500	0.075	0.046	6,400
16	10	800	10	7.1	1.0	500	0.013	0.008	6,400
17†	10	200	10	7.1	1.0	500	0.17	0.13	6,400

Asterisk (*) denotes a prescribed constant overall mass flowrate (as opposed to a constant flow velocity) for varied inlet diameters d_{sl}; dagger (†) denotes large eddy simulation (LES) turbulent model as a comparison case. Parameters not specified conform to base-case conditions. Calculated values are reported to two significant figures at most. See Eq. S4 and surrounding description in SI for definition of Re_{max}

effectively constant for $r/R < 0.8$, suggesting that flame speed measurements taken in this field of view would feature highly homogeneous, spatially uniform turbulence and flow fields. For $r/R > 0.8$ (i.e., near the chamber wall), viscous dissipation likely damps the turbulent fluctuations and leads to observable deviations in index profiles; these wall effects are more pronounced for lower frequencies, which necessarily feature longer timescales for turbulent fluctuation settling. Overall, while turbulence descriptors here do not yet match or exceed the magnitudes of those predicted for traditional jets (Davani and Ronney 2017), the model framework instead serves to illustrate that synthetic jets may indeed be capable

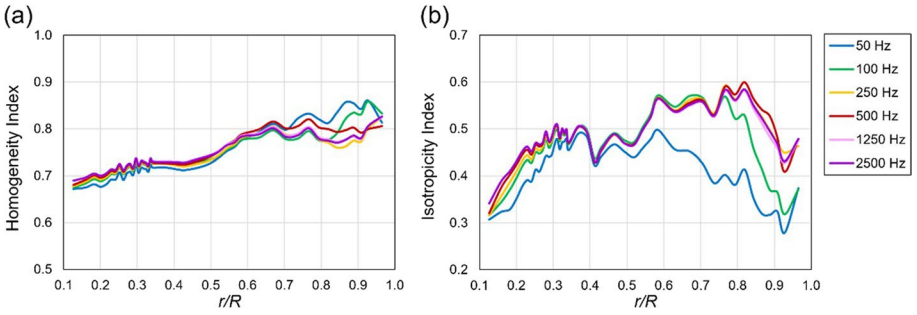

Fig. 3 Spatial variability of **a** HI and **b** II values along the dimensionless radial coordinate r/R calculated for various oscillation frequencies. See Table 1 for baseline conditions and Eqs. 3–4 for definitions

of generating spatially uniform turbulence (Figs. 2–3, S2) at sufficient intensities relevant to CVCC-based experiments (Fig. S6, Table 2).

Temperature and pressure also impact predicted turbulence profiles by changing effective fluid densities, and thus momentum flux. Simulation results of stoichiometric fluid mixtures initially at 600 K, 30 atm or both are summarized in Table S2. While elevated temperature increases the magnitude of calculated mean and RMS velocities, system pressure indeed has a pronounced retardation effect on turbulent fields. However, MFI, HI and II are generally lower for these cases, suggesting hypothetical CVCC experiments with denser fluids may feature highly uniform turbulence at elevated pressures. Additionally, future synthetic jet studies with well-defined cavity geometries and heated chamber walls may reveal heat transfer enhancements for pre-experiment thermal equilibration.

Finally, beyond the effects of slit diameter (Table 2, Nos. 2, 11–14), we assess the geometric impact of the total number of jets N. We construct new hypothetical chambers containing 4 and 20 symmetrically placed synthetic jets and compare them at Table 1 conditions, for cases of both constant flow velocity and constant mass flowrate (Table S3, Fig. S7). For the $N=20$ case at constant flow velocity, values of u' as high as 0.53 $\mathrm{m{\cdot}s^{-1}}$ are achieved, although practical constraints such as placement of optical windows may prohibit such a large N in a real device. Nonetheless, these results illustrate the numerous important, flexible design handles available to researchers seeking to construct a synthetic jet-agitated CVCC in the future.

3 Conclusions

Synthetic jets are demonstrated to be a new, potentially promising turbulence generation device for CVCCs, and the model framework established here allows for initial testing of important fundamental and practical design hypotheses. These devices and their prospective applications warrant further investigation from the combustion community, particularly on fundamental mixing physics, cavity design, slit geometry, vibrational mechanisms and phasing, suitable materials, device scaling relationships and safety considerations.

Supplementary Information The online version contains supplementary material available at https://doi.org/10.1007/s10494-023-00410-9.

Acknowledgements This work was authored by the National Renewable Energy Laboratory, operated by Alliance for Sustainable Energy, LLC, for the U.S. Department of Energy (DOE) under Contract No. DE-AC36-08GO28308. This work was supported by the Laboratory Directed Research and Development (LDRD) Program at NREL. N.E.T. and B.T.Z. thank Jason Lustbader and Gilbert Moreno for their helpful conversations and guidance. The views expressed in the article do not necessarily represent the views of the DOE or the U.S. Government. The U.S. Government retains and the publisher, by accepting the article for publication, acknowledges that the U.S. Government retains a nonexclusive, paid-up, irrevocable, worldwide license to publish or reproduce the published form of this work, or allow others to do so, for U.S. Government purposes.

Author contributions N.E.T. and X.F. co-wrote the main manuscript text and co-prepared all figures and tables with equal contribution. B.T.Z. and N.E.T. conceived of the synthetic jets concept for turbulent flame speed measurements. B.T.Z. mentored N.E.T., outlined the manuscript and gathered references. S.N. and S.Y. mentored X.F. in designing synthetic jet simulations and assessing model sensitivity. S.N. and M.S.D. reviewed model assumptions, equations, simulation execution and results. N.E.T. led the study and managed all author activities and contributions. All authors reviewed and approved of the final manuscript.

Funding Open access funding provided by National Renewable Energy Laboratory Library. This work was supported by the Laboratory Directed Research and Development (LDRD) Program at the National Renewable Energy Laboratory (NREL).

Declarations

Competing interests The authors declare no competing interests.

Ethical approval Not applicable. The research did not involve human or animal participants.

Informed consent Not applicable. The research did not involve human participants.

References

Arik, M., Sharma, R., Lustbader, J., and He, X.: Comparison of synthetic and steady air jets for impingement heat transfer over vertical surfaces. In: 13th InterSociety Conference on Thermal and Thermomechanical Phenomena in Electronic Systems pp. 1354-1363 (2012). https://doi.org/10.1109/ITHERM.2012.6231578.

Bagdanavicius, A., Bowen, P.J., Bradley, D., Lawes, M., Mansour, M.S.: Stretch rate effects and flame surface densities in premixed turbulent combustion up to 1.25 MPa. Combust. Flame **162**(11), 4158–4166 (2015)

Bonhomme, A., Duchaine, F., Wang, G., Selle, L., Poinsot, T.: A parallel multidomain strategy to compute turbulent flows in fan-stirred closed vessels. Comput. Fluids **101**, 183–193 (2014). https://doi.org/10.1016/j.compfluid.2014.06.010

Bradley, D., Lawes, M., Liu, K., Mansour, M.S.: Measurements and correlations of turbulent burning velocities over wide ranges of fuels and elevated pressures. Proc. Combust. Inst. **34**(1), 1519–1526 (2013). https://doi.org/10.1016/j.proci.2012.06.060

Bradley, D., Lawes, M., Morsy, M.E.: Measurement of turbulence characteristics in a large scale fan-stirred spherical vessel. J. Turbul. **20**(3), 195–213 (2019). https://doi.org/10.1080/14685248.2019.1610566

Capuano, F., Palumbo, A., de Luca, L.: Comparative study of spectral-element and finite-volume solvers for direct numerical simulation of synthetic jets. Comput. Fluids **179**, 228–237 (2019). https://doi.org/10.1016/j.compfluid.2018.11.002

Chaudhari, M., Verma, G., Puranik, B., Agrawal, A.: Frequency response of a synthetic jet cavity. Exp. Thermal Fluid Sci. **33**(3), 439–448 (2009). https://doi.org/10.1016/j.expthermflusci.2008.10.008

Chaudhari, M., Verma, G., Baramade, A., Puranik, B., and Agrawal, A.: Near-Field Measurements and Cavity Design for Synthetic Jets. In: 38th Fluid Dynamics Conference and Exhibit.) (2008)

Daniele, S., Jansohn, P., Mantzaras, J., Boulouchos, K.: Turbulent flame speed for syngas at gas turbine relevant conditions. Proc. Combust. Inst. **33**(2), 2937–2944 (2011). https://doi.org/10.1016/j.proci.2010.05.057

Davani, A., Zhou, Z., and Ronney, P.: CFD Deign of Jet-Stirred Reactors. In: AIAA Scitech 2019 Forum.) (2019)

Davani, A.A., Ronney, P.D.: A jet-stirred chamber for turbulent combustion experiments. Combust. Flame **185**, 117–128 (2017). https://doi.org/10.1016/j.combustflame.2017.07.009

Farrell, J.T., Johnston, R.J., Androulakis, I.P.: Molecular structure effects on laminar burning velocities at elevated temperature and pressure. SAE Trans. (2004). https://doi.org/10.4271/2004-01-2936

Han, K., Lee, H., Hwang, W.: Pseudo real-time continuous measurements of particle preferential concentration in homogeneous isotropic turbulence. Exp. Therm. Fluid. Sci. **112**, 109968 (2020)

Hassan, A.A., JanakiRam, R.D.: Effects of Zero-Mass "Synthetic" Jets on the Aerodynamics of the NACA-0012 Airfoil. J. Am. Helicopter Soc. **43**(4), 303–311 (1998). https://doi.org/10.4050/JAHS.43.303

He, X., Lustbader, J.A., Arik, M., Sharma, R.: Heat transfer characteristics of impinging steady and synthetic jets over vertical flat surface. Int. J. Heat Mass Transf. **80**, 825–834 (2015). https://doi.org/10.1016/j.ijheatmasstransfer.2014.08.006

Hwang, W., Eaton, J.K.: Creating homogeneous and isotropic turbulence without a mean flow. Exp. Fluids **36**(3), 444–454 (2004). https://doi.org/10.1007/s00348-003-0742-6

Jain, M., Puranik, B., Agrawal, A.: A numerical investigation of effects of cavity and orifice parameters on the characteristics of a synthetic jet flow. Sens. Actuators, A **165**(2), 351–366 (2011). https://doi.org/10.1016/j.sna.2010.11.001

Kotapati, R.B., Mittal, R., Cattafesta Iii, L.N.: Numerical study of a transitional synthetic jet in quiescent external flow. J. Fluid Mech. **581**, 287–321 (2007). https://doi.org/10.1017/S0022112007005642

Kral, L., Donovan, J., Cain, A., and Cary, A.: Numerical simulation of synthetic jet actuators. In: 28th AIAA Fluid Dynamics Conference. 1824 (1997)

Law, C.K.: Combustion physics. Cambridge University Press, Cambridge (2006)

Mahalingam, R., Glezer, A.: Design and thermal characteristics of a synthetic jet ejector heat sink. J. Electron. Packag. **127**(2), 172–177 (2004). https://doi.org/10.1115/1.1869509

Mannaa, O.A., Mansour, M.S., Chung, S.H., Roberts, W.L.: Characterization of turbulence in an optically accessible fan-stirred spherical combustion chamber. Combust. Sci. Technol. (2019). https://doi.org/10.1080/00102202.2019.1686629

Marshall, A., Lundrigan, J., Venkateswaran, P., Seitzman, J., and Lieuwen, T.: Measurements of Stretch Statistics at Flame Leading Points for High Hydrogen Content Fuels. Journal of Engineering for Gas Turbines and Power, 139(11), (2017). https://doi.org/10.1115/1.4035819

Matiz-Chicacausa, A., Lopez Mejia, O.D.: Towards accurate boundary conditions for cfd models of synthetic jets in quiescent flow. Energies **13**(24), 6514 (2020)

Mautner, T.: Application of the synthetic jet concept to low Reynolds number biosensor microfluidic flows for enhanced mixing: a numerical study using the lattice Boltzmann method. Biosens. Bioelectron. **19**(11), 1409–1419 (2004). https://doi.org/10.1016/j.bios.2003.12.023

McCormick, D.: Boundary layer separation control with directed synthetic jets. In: 38th Aerospace Sciences Meeting and Exhibit (2000)

Morones, A., Turner, M.A., León, V., Ruehle, K., and Petersen, E.L.: Validation of a new turbulent flame speed facility for the study of gas turbine fuel blends at elevated pressure. ASME Turbo Expo 2019: Turbomachinery Technical Conference and Exposition Volume 4A: Combustion, Fuels, and Emissions, (2019) https://doi.org/10.1115/gt2019-90394

Ravi, S., Peltier, S.J., Petersen, E.L.: Analysis of the impact of impeller geometry on the turbulent statistics inside a fan-stirred, cylindrical flame speed vessel using PIV. Exp. Fluids **54**(1), 1424 (2012). https://doi.org/10.1007/s00348-012-1424-z

Roache, P.J.: Perspective: a method for uniform reporting of grid refinement studies. J. Fluids Eng. **116**(3), 405–413 (1994). https://doi.org/10.1115/1.2910291

Smith, B.L., Swift, G.W.: A comparison between synthetic jets and continuous jets. Exp. Fluids **34**(4), 467–472 (2003). https://doi.org/10.1007/s00348-002-0577-6

Turner, M.A., Paschal, T., Kulatilaka, W.D., and Petersen, E.L.: An Investigation of Laminar Flame Speed of CH4-O2-CO2 Mixtures. ASME Turbo Expo 2019: Turbomachinery Technical Conference and Exposition Volume 4B: Combustion, Fuels, and Emissions. (2019). https://doi.org/10.1115/gt2019-91392.

Authors and Affiliations

Nicholas E. Thornburg[1] · Xuhui Feng[1] · Bradley T. Zigler[1] · Marc S. Day[2] · Shashank Yellapantula[2] · Sreekant Narumanchi[1]

[1] Center for Integrated Mobility Sciences, National Renewable Energy Laboratory, 15013 Denver West Parkway, Golden, CO 80401-3305, USA

[2] Computational Science Center, National Renewable Energy Laboratory, 15013 Denver West Parkway, Golden, CO 80401-3305, USA